Absolute Spin Assignments of Dy^{161} and Dy^{163} Neutron Resonances and the Hyperfine Coupling Constants in Dy^{163}

G. BRUNHART, HANS POSTMA †, D. C. RORER, V. L. SAILOR, and L. VANNESTE ‡

Brookhaven National Laboratory, Upton, New York

(Z. Naturforsch. **26 a**, 334—342 [1971]; received 7 December 1970)

Dedicated to Prof. Dr. H. Maier-Leibnitz on his 60th birthday

A method and equipment are described for measuring the spin dependence of slow neutron cross sections. The neutron beam from the High Flux Beam Reactor (HFBR) is polarized by Bragg reflection from a magnetized 92% Co-8% Fe single crystal which process also serves to select the neutron energy. Nuclei in the target are statically polarized in a field of ~ 35 kOe at temperatures ranging from 0.05 to 0.10 K. Large nuclear polarizations are obtained in polycrystalline ferromagnetic dysprosium metal because of the large magnetic hyperfine interaction. The total angular momenta, J, of the compound states corresponding to the first several resonances in Dy^{161} and Dy^{163} were determined by measuring the transmission of the target with the neutron beam alternately polarized parallel and antiparallel to the nuclear polarization. Quantitative results at two resonances of opposite spin permit absolute J-value assignments (i. e., the assignments are independent of any knowledge of the absolute signs of the nuclear magnetic moments).

Results were as follows:

Isotope	163	161	161	161	161	161	161	161	161	163	161	161
E_0 (eV)	1.71	2.72	3.69	4.35	7.75	10.40	10.87	12.65	14.3	16.25	16.7	18.5
J	2	3	2	2	3	2	3	2(?)	2	3	(?)	2

The hyperfine interaction constants for Dy^{163}, obtained by measuring the nuclear polarization as a function of temperature, were $A/k=0.100\pm0.005$ K, and $P/k=0.008\pm0.001$ K where A and P are, respectively, the magnetic and the electric hyperfine interaction constants.

I. Introduction

The interaction of polarized neutrons with polarized nuclei provides relatively direct information about the spin dependence of neutron cross sections, and the spin of compound states corresponding to neutron resonances. In addition, measurements with polarized systems can yield reasonably accurate values for the magnetic hyperfine interaction particularly in ferromagnetic solids. From 1961 to 1967, we conducted a variety of such experiments [1] at the Brookhaven Graphite Research Reactor (BGRR). Although a curtailment in BGRR operations forced a suspension of the program in 1967, a similar program has been initiated recently at the High Flux Beam Reactor (HFBR). The new facility should ultimately provide superior experimental conditions; i. e. higher neutron intensity over an expanded energy interval, better neutron energy resolution, lower target temperatures, and more intense magnetic fields for target polarization. In this paper we shall present some of the first results obtained with the new equipment and give a brief description of the system.

Dysprosium was selected as our first target because work at BGRR on this element was incomplete [2] yet enough data had been collected to allow a good comparison between the two facilities.

* Work supported by the U.S. Atomic Energy Commission.

† Guest from Kamerlingh Onnes Laboratorium, Leiden; present address: Natuurkundig Laboratorium Rijks-Universiteit, Groningen, The Netherlands.

‡ Guest from Instituut voor Kern- en Stralingsfysika, Katholieke Universiteit Leuven, Belgium.

[1] A representative selection can be found in the following papers: H. MARSHAK, H. POSTMA, V. L. SAILOR, F. J. SHORE, and C. A. REYNOLDS, Phys. Rev. **128**, 1287 [1962]. — G. BRUNHART, H. POSTMA, and V. L. SAILOR, Phys. Rev. **137**, B 1484 [1965]. — L. PASSELL and R. I. SCHERMER, Phys. Rev. **150**, 146 [1966]. — R. I. SCHERMER, Phys. Rev. **130**, 1907 [1963]. — R. I. SCHERMER, L. PASSELL, G. BRUNHART, C. A. REYNOLDS, V. L. SAILOR, and F. J. SHORE, Phys. Rev. **167**, 1121 [1968].

[2] G. BRUNHART, H. MARSHAK, C. A. REYNOLDS, V. L. SAILOR, R. I. SCHERMER, and F. J. SHORE, Bull. Amer. Phys. Soc. II, **7**, 305 [1962]. — G. BRUNHART, Proc. Sixth Rare Earth Research Conf., Gatlinburg, Tenn., May 3—5, 1967, pp. 495—505, ORNL Publ. 1967.

Since the Dy neutron cross section contains many closely spaced resonances [3] it provides a challenging case for study.

Large nuclear polarization can be achieved in Dy^{161} and Dy^{163} by utilizing the large magnetic hyperfine interaction which results primarily from the unpaired $4f$ electrons.

Although both Dy^{161} and Dy^{163} have spin $I=5/2$, the magnetic moments are opposite in sign [4, 5], consistent with the classification of the ground state configurations of MOTTELSON and NILSSON [6]. Various arguments [4–6] indicate that the absolute signs of the moments are: Dy^{161} negative, Dy^{163} positive. Our results verify such an assignment as will be discussed later. Some of the nuclear properties of the Dy isotopes are summarized in Table I.

Table 1. Some properties of Dy^{161} and Dy^{163}.

Isotope	Isotopic Abundance	Nuclear Spin	Nuclear Magnetic Dipole Moment
Dy^{161}	18.88	5/2	$-0.47\,\mu_N$
Dy^{163}	24.97	5/2	$+0.66\,\mu_N$

Dysprosium metal becomes ferromagnetic below ~ 87 K [7]. The ferromagnetism is strongly anisotropic with the moments lying in the basal plane of the hcp crystal lattice. The polycrystalline metal does not magnetically saturate even in fields as large as 80 kOe [8]. At 1.5 K and ~ 40 kOe Henry observed a magnetization of $\sim 74\%$ of saturation, if the saturation moment is 10 Bohr magnetons. (Recent data at liquid helium temperatures indicate that polycrystalline Dy might have a lower saturation value than for a single crystal. [9]) There is evidence that in single crystals the 4.2 °K and 20.4 °K magnetic moment isotherme lie below the 31.2 K isotherm [10]. This might be attributed to the reappearance of some modified antiferromagnetism at the lower temperatures [11] since the population of some lower moment electronic state seems to be inconsistent with specific heat data. Thus the existing information strongly suggests some modified ferromagnetic structure at helium temperatures but the exact nature is unknown.

II. Method

A) Measurement of the Transmission Effect

The principal experiment consists of measuring the transmission of a polarized monoenergetic neutron beam through a target in which the nuclear spin system is partially polarized. This is done with the neutron polarization alternately parallel and antiparallel to the magnetic field applied to the target. Such measurements are repeated as a function of neutron energy and of target temperature (i. e. target polarization).

We have previously shown [12] that a useful experimental quantity is the transmission *effect*, $\mathcal{E}$, defined as:

$$\mathcal{E} \equiv \frac{\mathcal{T}_P-\mathcal{T}_A}{\mathcal{T}_P+\mathcal{T}_A} = \frac{C_P-C_A}{C_P+C_A-2B}, \quad (1)$$

where $\mathcal{T}_{P,A}$ are the transmissions in the parallel and antiparallel configurations, $C_{P,A}$ are the counting rates after transmission through the target for the two respective configurations and B is the background counting rate. Neglecting neutron energy resolution and beam depolarization, it can be shown [12] that

$$\mathcal{E} = -\tfrac{1}{2}(1+\varphi)\, f_n{}^0 \tanh(N\, t\, \sigma\, \varrho\, f_N), \quad (2)$$

where φ is the efficiency for reversing the neutron spin to the antiparallel configuration, $f_n{}^0$ is the incident neutron polarization, N the density of target nuclei, t the target thickness, σ the total cross section, ϱ a statistical weighting factor, and f_N the nuclear polarization. When viewing a strong well-

[3] V. L. SAILOR, H. H. LANDON, and H. L. FOOTE, JR., Phys. Rev. **96**, 1014 [1954]. — R. L. ZIMMERMANN, Bull. Amer. Phys. Soc. II, **2**, 42 [1957]. — S. F. MUGHABGHAB, A. P. JAIN, and R. E. CHRIEN, Bull. Amer. Phys. Soc. II, **9**, 433 [1964]. — Resonance parameters are summarized in Neutron Cross Sections, BNL 325, 2nd Ed. Supplement No. 2, Vol. II C, $Z=61$ to 87, Brookhaven National Laboratory, August 1966.

[4] J. G. PARK, Proc. Roy. Soc. London A **245**, 118 [1958].

[5] E. EBENHÖH, V. J. EHLERS, and J. FERCH, Z. Physik **200**, 84 [1967].

[6] B. R. MOTTELSON and S. G. NILSSON, Mat. Fys. Skr. Dan. Vid. Selsk. **1**, 105 [1959].

[7] M. K. WILKINSON, W. C. KOEHLER, E. O. WOLLAN, and J. W. CABLE, J. Appl. Phys. **33**, Suppl. 48 S [1962].

[8] W. E. HENRY, J. Phys. Radium **20**, 1962 [1959].

[9] B. G. LAZAREV, L. S. LAZAREVA, and S. I. GORIDOV, Dokl. Akad. Nauk SSSR **183**, 1295 [1968].

[10] J. F. ELLIOTT, S. LEGVOLD, and F. H. SPEDDING, Phys. Rev. **94**, 1143 [1954].

[11] F. H. SPEDDING, S. LEGVOLD, A. H. DAANE, and L. D. JENNINGS, Progress in Low Temperature Physics, Vol. II, pp. 368—394 (edited by C. J. GORTER), North-Holland Publishing Co., Amsterdam 1957.

[12] H. POSTMA, H. MARSHAK, V. L. SAILOR, F. J. SHORE, and C. A. REYNOLDS, Phys. Rev. **126**, 979 [1962].

resolved resonance in the cross section it is often a good approximation to assume that σ is due entirely to this resonance. However, our routine data analysis program uses a more complicated version of Eq. (2) which also takes into account neutron energy resolution, Doppler broadening, beam depolarization and overlap of two or more resonances:

$$\langle \mathcal{E} \rangle = -\tfrac{1}{2}(1+\varphi)\, f_{\mathrm{n}}{}^{0} \cdot \frac{\int R(E-E')\, \tau\, e^{-\alpha t} \sinh(\varkappa t)\, \mathrm{d}E'}{\int R(E-E')\, e^{-\alpha t}\{\cosh(\varkappa t) + [\nu - \tfrac{1}{2}(1-\varphi)\, \tau\, f_n{}^{0}] \sinh(\varkappa t)\}\, \mathrm{d}E'}, \quad (3)$$

where $R(E-E')$ is the spectrometer resolution function; $\alpha = N\sigma + D$ (with D being the depolarization factor); $\varkappa = (N^2 \sigma^2 p^2 + D^2)^{1/2}$ with $p = \varrho f_{\mathrm{N}}$; $\tau = N\sigma p/\mathrm{k}$ and $\nu = D/\mathrm{k}$.

B) Spin Assignments of Resonances

Since slow neutron resonances are limited to s-wave interactions, the compound state which is formed can have only two alternative values of total angular momentum, $J = I + \frac{1}{2}$ or $J = I - \frac{1}{2}$, where I is the target ground state spin. Corresponding to these two alternative J-values the statistical factor in Eq. (2) has the two possible values, $\varrho_{+} = I/(I+1)$ and $\varrho_{-} = -1$. Thus each slow neutron resonance is characterized by one or the other value of ϱ. If the *transmission effect*, $\mathcal{E}$, is measured at a neutron energy for which the cross section is predominately due to a single resonance, the sign of $\mathcal{E}$ immediately yields the sign of ϱ and thus J, provided the absolute sign of the nuclear polarization f_{N} is known.

In many cases the absolute sign of f_{N} is in fact not known because of uncertainties in the absolute sign of the magnetic hyperfine interaction constant, i. e. either H_{eff} or μ. For example, it is reasonable that H_{eff} is + for both Dy^{161} and Dy^{163} because the large magnetic hyperfine interaction must be a consequence of the unpaired $4f$ electrons. However, the sign determination of the two magnetic moments is less certain, and the sign of f_{N} for each isotope reflects this uncertainty. One useful result of the neutron measurements is that even in this situation there is the possibility of obtaining absolute values of ϱ which in turn yield the absolute sign of f_{N} and of the product μH_{eff}. This absolute determination can be made by comparing the magnitude of $\mathcal{E}$ at various resonances.[13]

C) Determination of Hyperfine Interactions

Once the ϱ value; i. e., J, at a fixed neutron resonance energy has been determined one can use the measurement of $\mathcal{E}$ as a function of the temperature T to yield the relationship between f_{N} and T using Eq. (3). The shape of the curve describing f_{N} as a function of $1/T$ is determined by the magnetic and electric hyperfine interaction constants. Thus, the experimental curves can be fitted[13, 14] with these constants as fitting parameters to obtain quantitative values of the hyperfine interaction.

III. Equipment

A) The Neutron Spectrometer

Monoenergetic polarized neutrons are obtained by Bragg reflection from a magnetized single crystal of 92% Co – 8% Fe alloy. The crystal is cut so that either the (111) or the (220) reflection can be used readily. The spectrometer is a two axis instrument which is sturdy enough to carry the heavy experimental components and is of large dimension to provide adequate space along the neutron path to accommodate all necessary collimators, slit systems, etc. Despite the massive construction, the instrument is capable of very high precision (±3 secs arc) in setting an angle. Such precision is necessary for working at neutron energies in excess of 10 eV since the Bragg angles become very small. A full description of the spectrometer is given elsewhere[15]. A schematic of the general layout is shown in Fig. 1.

The neutron energy resolution is determined by the grating space of the crystal planes and by the collimating system[16]. A selection of several collimators are available for use up- and down-stream from the monochromator so that the resolution can be varied as needed. At present the best resolution is ~2.5′ arc, which at 10 eV with the (220) reflection yields a resolution width of 0.4 eV.

B) Neutron Polarization

The neutron polarization leaving the crystal is in the range of 0.90 to 0.92. The polarized beam must remain in a small but finite magnetic field along its entire path to avoid depolarization. Our "guide" field has several sections which are listed in Table 2. With the exception of the rotator, these fields are approximately vertical. The presence of small horizontal field components cannot be avoided but can contribute to appreciable beam depolarization. It is necessary to measure the beam polarization as a function of neutron velocity and strength of the various fields to obtain

[13] G. Brunhart and V. L. Sailor, Phys. Rev. **2 C**, 1137 [1970].

[14] G. Brunhart, H. Postma, and V. L. Sailor, Phys. Rev. **137**, B 1484 [1965].

[15] H. L. Foote, Jr., and V. L. Sailor, Rev. Sci. Instr. (to be submitted).

[16] V. L. Sailor, H. L. Foote, Jr., H. H. Landon, and R. E. Wood, Rev. Sci. Instr. **27**, 26 [1956].

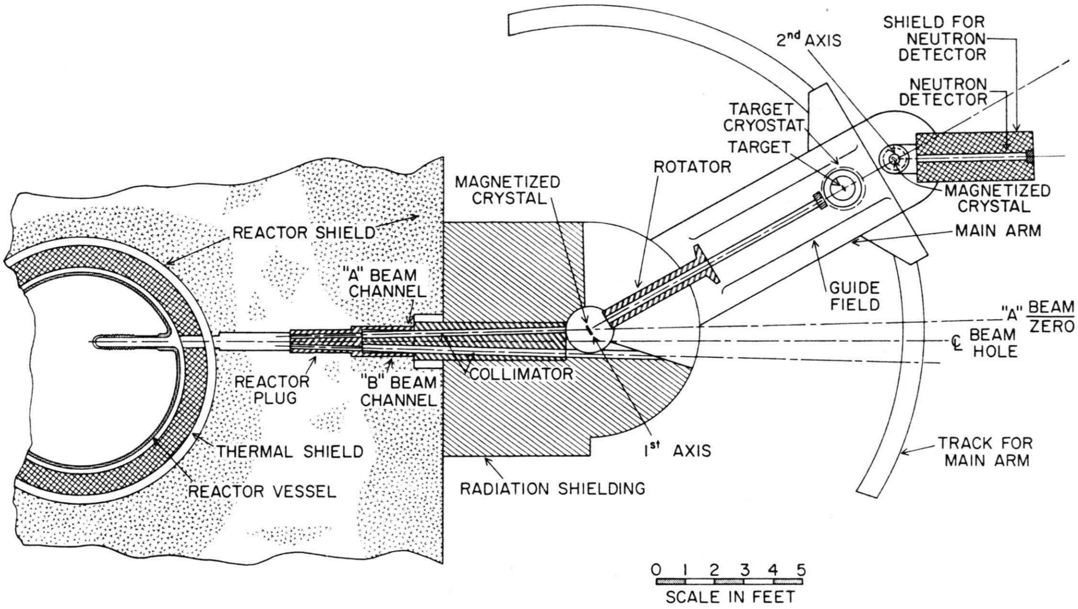

Fig. 1. Schematic diagram of the neutron spectrometer. The neutron energy is selected at the first axis by Bragg reflection which also serves to polarize the beam. The polarization can be inverted in the "rotator". The beam polarization is analyzed by Bragg reflection on the second axis. To obtain maximum energy resolution an additional collimator is inserted between the target cryostat and the neutron detector.

the optimum adjustments. The beam polarization is measured by observing the Bragg reflection in parallel and antiparallel configuration from a second magnetized Co – Fe cyrstal similar to the monochromating crystal. The second axis of the spectrometer allows this to be done conveniently. The lower energies (< 0.5 eV) seem to be more susceptible to depolarization, and hence the field settings more critical. Although this situation needs more exhaustive investigation it now appears that a combination of settings has been found for which the beam polarization is essentially energy independent.

In most measurements it is necessary to reverse the neutron spin between alternate counts. This reversal is accomplished in the "rotator" section. The rotator is a cylindrical stainless steel shielding plug having two sets of windings which can be energized alternately. One set is straight and delivers the neutrons to the Arm Guide Section with spin UP. The other set of windings make a 180° spiral along the length of the plug and delivers the neutrons to the Arm Guide Section with spin DOWN. The field is strong enough and the spiral pitch is long enough so that the neutron spin adiabatically follows the gradual change of field

Table 2. Elements of magnetic fields along neutron path which maintain the beam polarization. The distances listed are from the crystal monochromator which polarizes the beam.

Section	Source of Field	Distance (inches)	Nominal Field (oersteds)	Direction of Field
1. Beam Polarizer Leakage Field	Permanent Magnet	0 to 12	8,000 → 160	Up
2. Transition	Permanent Magnets	12 to 22	160 → 22	Up
3. Rotator	Straight Coils	22 to 55	22	Up
or				or,
{3. Rotator	Helical Coils	22 to 55	{ 22	Up spiraling to down
{4. Flip Foil	Current "foil"	55	{ 22 Down → 12 Up	Discontinuity
5. Arm Guide	Coils	55 to 110	12	Up
6. Target Magnet	Leakage from iron yoke	110 tp 120	12 → 600	
7. Target Magnet Yoke to Windings	Superconducting split solenoid in iron jacket	120 to 122	600 up to 35,000 down	Inverts
8. At Target	Center of target magnet	125	35,000	Down

direction. When the spiral windings are energized, current is passed through a "flip foil" to give a sudden 180° reversal of field direction as the neutrons pass from the rotator into the arm guide section. The "flip foil" consists of a flat sheet of 0.010 cm diameter copper wires tightly spaced, wound in series with a wide return loop. This provides an effective DC current sheet in the horizontal direction. The field from this current sheet is DOWN on the rotator side and UP on the Arm Guide side. Since the time required for the neutrons to pass through this "foil" is short compared to a Larmor period, they can transmigrate the field reversal without flipping their spins. In order for the flip foil to work effectively, the fields from the end of the rotator (spiral windings) and the Arm Guide coil must cancel to zero at the center of the flip coil.

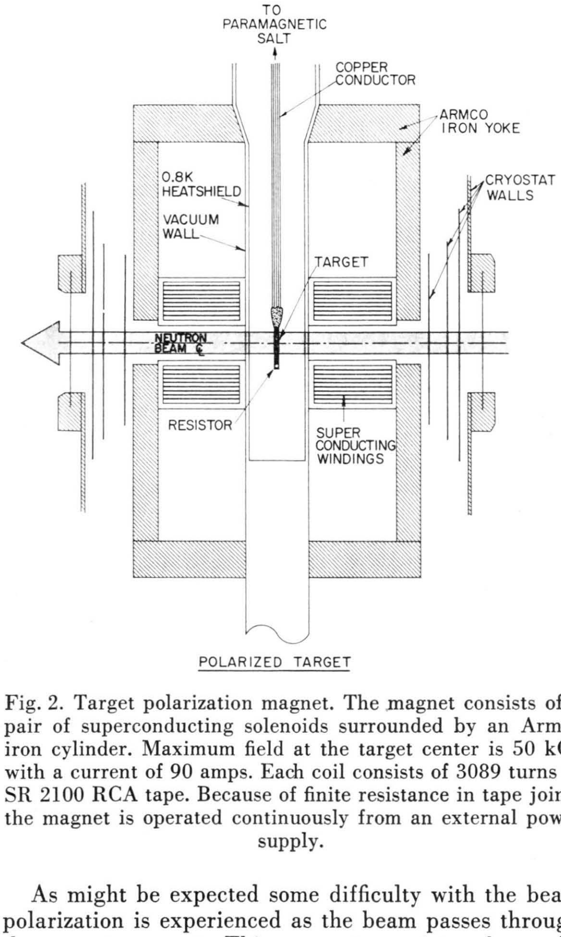

Fig. 2. Target polarization magnet. The magnet consists of a pair of superconducting solenoids surrounded by an Armco iron cylinder. Maximum field at the target center is 50 kOe with a current of 90 amps. Each coil consists of 3089 turns of SR 2100 RCA tape. Because of finite resistance in tape joints the magnet is operated continuously from an external power supply.

As might be expected some difficulty with the beam polarization is experienced as the beam passes through the target magnet. This magnet consists of a split pair of superconducting solenoids surrounded by an iron jacket (see Fig. 2). Because of space limitations in the cryostat the thickness of the iron jacket is limited to ½ inch with an outside diameter of 6.5 inches. Consequently at higher fields the return flux saturates the iron which results in considerable flux leakage in the region where the beam approaches and leaves the cryostat (~600 oersted at the cryostat windows). The solenoid is magnetized so that this leakage field is parallel to the arm guide field. Apparently the beam polarization is not adversely affected as it enters or leaves the cryostat. However, inside the iron jacket, between the jacket and the outside diameter of the superconducting windings, the beam must pass through a very strong gradient which, except for the center plane, has a large radial component. If the two halves of the solenoid are producing equal fields, neutrons traversing the central plane pass through without flipping their spins, but neutrons above and below are adiabatically turned over by the strong radial gradient in entering and again in leaving. Thus the net beam polarization at the target can be very small even though the polarization after passing through the magnet is large. In addition, neutron trajectories which have an appreciable vertical component can result in a flip while entering but not in leaving and vice versa. These latter events contribute to the depolarization of the neutron beam. These effects have been observed directly by sampling various parts of the beam while measuring both a transmission effect and the polarization of the neutron beam.

A method for avoiding the central plane "polarization catastrophe", is to energize the two halves of the magnet differently. This moves the plane of magnetic symmetry above or below the beam. When the current in the two halves of the magnet is about 20% different all neutrons flip 180° before entering the target and flip back again after leaving. Typical currents used in the top/bottom windings were 56/70 amps which give a field of ~35 kOe at the center of the target. Although this works well at moderately high fields, it is not an ideal mode of operation because it places the target in a strong field gradient which causes extremely strong forces on ferromagnetic samples. Furthermore, the effective field on the target is considerably less than the maximum field that the split solenoid could produce with equal currents.

Probably the best way to eliminate the difficulties mentioned above would be to provide an additional set of windings inside the magnet gap to insure that all neutrons behave in the same manner. The design and installation of such a coil is not a trivial matter although we hope ultimately to incorporate such a device.

C) Superconducting Magnets and Power Supplies

The cryogenic magnet package used in this experiment consists of three superconducting solenoids, which will be referred to as magnets A, B, and C respectively. The A solenoid, which has a winding approximately 2.5 in. long, is used to provide fields up to 2 kOe in a bore of 2 in. diameter, for the purpose of activating a superconducting Pb heat switch. Magnet B, with a winding approximately 10.75 in. long, produces a field up to 25 kOe in a 2 in. diameter bore and is used to magnetize the refrigerating salt. Both A and B magnets are wound from 0.010 in. diameter NbZr wire and require 12 amperes and 20 amperes, respectively, to achieve full field strength.

Magnet C, used to polarize the sample, consists of a pair of coils separated by an axial gap of 0.875 in. to allow radial access to the neutron beam. These coils are wound with Nb_3Sn ribbon, 0.091 in. wide and 0.003 in. thick. A 90-ampere current in the windings produces a field of 50 kOe at the center of the magnet; this field does not vary by more than 4% over the axial gap.

Current for the magnets is obtained from programmable solid state D.C. power supplies[17] having a stability and regulation of 0.01%. An integrator circuit using an operational amplifier generates an extremely smooth varying ramp voltage to program the power supplies; this allowes the magnets to be turned on or off slowly and smoothly over a period of up to several hours, if desired.

Current leads inside the Dewar had to be designed to minimize the boil-off of liquid helium associated with the introduction of 100-ampere capacity wires into the bath. (Attempts to operate the magnets in the persistent mode were soon abandoned because of the gradual decay of persistent currents in the windings due to inevitable residual resistance at the joints of the wires. Continuous operation of the current leads was therefore necessary.) The current leads used consist of arrays of copper wires arranged so as to have a large surface area exposed to the cold gas evaporating from the liquid helium. The cross-sectional area of each lead is increased at the warm end by adding more wires to the array, while at the cold end, each lead is paralleled for some distance by a piece of superconducting ribbon to eliminate Joule heating of that part of the lead in direct contact with the bath.

Current supplied to each solenoid is monitored by a digital voltmeter connected across a 0.001 ohm resistor in series with each coil. The magnetic field was calibrated using a rotating coil Gaussmeter[18] operated at room temperature inside an "insert" Dewar which was placed in the bore of the solenoids. The Gaussmeter was capable of 0.1% accuracy in fields up to 100 kOe.

D) Target Refrigeration

The data yielding the hyperfine interaction constants were obtained several years ago at the BNL graphite reactor (BGRR). For these measurements the target was cooled indirectly by adiabatic demagnetization of a large paramagnetic salt. The salt crystals were grown on several thousand No. 36 copper wires the ends of which were silver soldered to a bundle of larger copper wires to which in turn the target was soldered. These target-salt assemblies gave excellent heat transport in the 0.04 K temperature range, and in metallic samples the nuclear spin system relaxation time was usually less than 1 minute[14]. The salt assembly consisted of two iron alum units separated by a Pb heat switch. The salts were demagnetized simultaneously, the upper salt serving to impede heat leakage and the lower salt serving as the low temperature reservoir. The upper unit was connected through a Pb heat switch to the main liquid helium bath maintained at ~ 0.90 K. Thus the vacuum walls surrounding the target were maintained at 0.90 K. In the course of many experiments over a period of several years the low temperature thermometry was refined to the necessary precision (for details see Ref.[1]).

Most of the spin assignments reported here were made at HFBR on the new spectrometer described in the previous two sections. Since these were among our first experiments with the new equipment, the refrigerator and thermometry were not nearly as well perfected. The main liquid helium bath which cooled the superconducting magnets was maintained at 4.2 K. The target assembly had a 500 cm^3 liquid helium bath at the top maintained at ~ 0.8 K by high speed pumping through a small aperture (to suppress the Rollin film). A potassium chrome alum salt was suspended from the small helium bath connected by a Pb heat switch. The target was suspended by copper conductors from the salt. To reduce heat transport from the surrounding 4.2 K walls, it was necessary to install a thin copper tube from the 0.8 K helium bath which enclosed the salt and target. The only thermometer consisted of a calibrated 100-ohm Speer resistor embedded in the target.

The lowest target temperatures achieved were about 0.05 K. After the adiabatic demagnetization data could be taken for 4 to 6 hours as the target warmed up to ~ 0.1 K.

IV. Results

A) Resonant Spin Assignments

The transmission, $\mathcal{T}$, and the transmision effect, $\mathcal{E}$, were measured as a function of neutron energy over the range from ~ 1 to ~ 20 eV at various temperatures between 0.05 and 0.15 K. At lower energies data were taken both at BGRR and HFBR so that the behavior of the neutron spin in passing through the HFBR superconducting split solenoid could be confirmed. Observed values of $\mathcal{E}$, depending on sample thickness, temperature and total cross section varied from 0 to $\sim 15\%$. Above 10 eV all data were obtained at HFBR using both Co(111) and Co(220) reflections, the latter giving better energy resolution but smaller neutron polarization ($f_n^0 \approx 0.80$).

[17] Kepco KS series power supplies, Kepco, Inc., Flushing, N.Y.

[18] Rawson-Lush Type 829 M 29 R. C. Gaussmeter, Rawson Electrical Instrument Co., Cambridge, Mass.

The data at the two lowest resonances, 1.71 eV (Dy^{163}) and 2.72 eV (Dy^{161}) were analyzed to obtain absolute values of ϱ based on the relative magnitudes of the observed transmission effects [13]. The effect $\langle \mathcal{E} \rangle$ was calculated over the range of these two resonances using the cross section of the first three resonances. Knowing the ratio of the nuclear magnetic moments of Dy^{161} and Dy^{163} and their relative sign and having measured the relative sign of the transmission effect for the first three resonances we have to distinguish between the two J-value combinations (2, 3, 2) and (3, 2, 3) for the first three resonances. The ratio of the calculated transmission effects at 1.71 eV and 2.73 eV for these two possibilities is $R_1 = 6.77$ and $R_2 = 4.04$. The experimentally determined ratio was $R_{\mathrm{exp}} = 6.4$ agreeing only with the first possibility. In this way the J-values for the first three resonances could be assigned absolutely and unambiguously. The knowledge of the J-values determined in this way can now be used to determine the sign of μH_{eff}, i. e. the sign of the nuclear polarization. The J-values of all other resonances were assigned relative to the first three. Results are summarized in Table III. Some of the data are shown in Fig. 3.

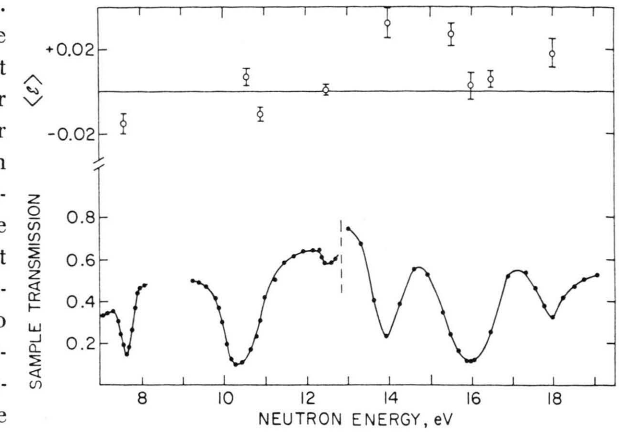

Fig. 3. Typical data. The lower curve shows the observed transmission, $\mathcal{T}$, as a function of neutron energy. The upper curve shows the observed transmission effect, $\langle \mathcal{E} \rangle$, as a function of neutron energy.

Table 3. Summary of spin assignments for Dy^{161} and Dy^{163} resonance. Total angular momentum, J, of compound state corresponding to resonance in cross section at E_0 can have the two possible values $J = I + \frac{1}{2}$ or $J = I - \frac{1}{2}$ where $I = 5/2$ the spin of the target nucleus.

Resonant Energy E_0 (eV)	Isotope	Observed J	Typical Observed Transmission Effects $\langle \mathcal{E} \rangle$ (Percent)	Note
1.71	163	2	$+12.30 \pm 0.30$	a
2.72	161	3	$+\ 4.10 \pm 0.30$	a
3.69	161	2	$-\ 7.90 \pm 0.40$	a
4.35	161	2	$-\ 4.75 \pm 0.40$	a
5.45	162	$\frac{1}{2}$	$+\ 0.30 \pm 0.50$	b
7.75	161	3	$(+) 3.14 \pm 0.94$	c
10.40	161	2	$(-) 1.35 \pm 0.08$	c
10.87	161	3	$(+) 2.06 \pm 0.75$	c
12.65	161	2 (?)	$(-) 0.60 \pm 0.80$	c,d
14.30	161	2	$(-) 6.46 \pm 1.40$	c
16.25	163	3	$(-) 5.48 \pm 0.01$	c
16.70	161	(?)	$(-) 0.60 \pm 2.00$	e
18.50	161	2	$(-) 3.50 \pm 1.18$	c

[a] Data taken in center plane of balanced magnet so neutrons enter target without flipping spin so sign of $\langle \mathcal{E} \rangle$ is correct.
[b] Nominal transmission effect, $\mathcal{E} = 0$, since Dy^{162} has spin $I = 0$ and hence no nuclear polarization. $J = \frac{1}{2}$ is only allowed compound spin.
[c] Data taken with unbalanced magnet, neutrons flip before entering target so correct sign of $\langle \mathcal{E} \rangle$ is opposite observed spin listed. The neutron flip was verified by taken data with both magnet conditions at several resonances.
[d] Assignment doubtful because resonance is very weak.
[e] No assignment possible due to overlap of much stronger Dy^{163} resonance at 16.25 eV.

It should be noted that the pairs of resonances at 10.40 and 10.87 eV, and at 16.25 and 16.7 eV could not be resolved. In the case of the 10 eV pair both spins could be assigned because the resonances were of similar strength and opposite sign so the observed $\mathcal{E}$ changed sign in passing through the unresolved transmission dip. However, in the case of the 16 eV pair only the stronger of the two at 16.25 eV could be assigned because the 16.7 eV resonance was relatively too weak to give an assignment within statistical uncertainty. The result for the weak resonance at 12.65 eV is also somewhat uncertain.

B) Hyperfine Interactions

The transmission effect $\langle \mathcal{E} \rangle$ at the 1.71 eV resonance was measured as a function of temperature. This data, shown in Fig. 4 establishes a relation between f_N, the nuclear polarization, and T, the absolute temperature of the sample. Describing the nuclear part of the hyperfine interaction by the spin Hamiltonian

$$\mathcal{H} = A\, S_z I_z + P[I_z^2 - \tfrac{1}{3} I(I+1)] \qquad (4)$$

where A and P are the magnetic and electric coupling constants, respectively, the nuclear polarization is given by

$$f_N = \frac{1}{I} \frac{\Sigma m \exp[-(\frac{1}{2} A\, m + P\, m^2)/k\, T]}{\Sigma \exp[-(\frac{1}{2} A\, m + P\, m^2)/k\, T]}\,. \qquad (5)$$

Using a least squares fit method we have fitted our data to Eq. (5) with A and P as fitting parameters.

The best fitting values are $A/k = 0.100 \pm 0.005$ K and $P/k = 0.008 \pm 0.001$ K. The solid curve in Fig. 4 was calculated using these values together with Eqs. (3) and (5).

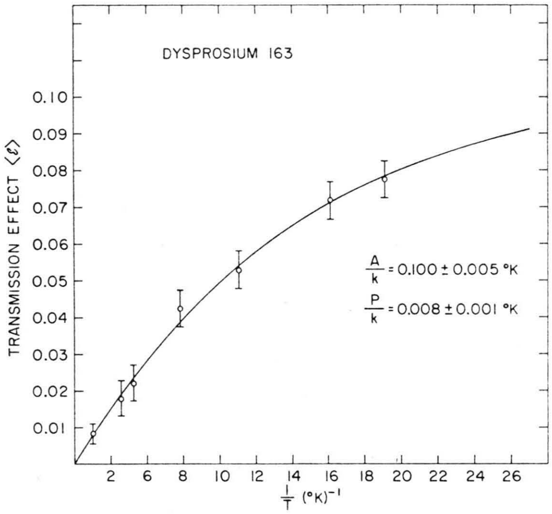

Fig. 4. Transmission effect, $\langle \mathcal{E} \rangle$, vs. inverse of target temperature for 1.71 eV resonance in Dy^{163}. The observed $\langle \mathcal{E} \rangle$ is proportional to the nuclear polarization. By fitting the data the magnetic, A/k, and electric quadrupole, P/k, interaction constants are derived.

V. Discussion

The spins of eleven compound states due to slow neutron resonances in Dy^{161} and Dy^{163} have been determined absolutely. The spin assignments are made on the basis of direct measurements and are independent of any assumption about the sign of the nuclear magnetic moments (other than the ratio of these moments) or the effective magnetic field at the nuclei. The results are summarized in Table III.

The hyperfine coupling constants A/k and P/k are directly related to effective magnetic and electric fields at the site of the nucleus. In the case of the rare earths these fields are determined mostly by the configuration of the $4f$ electrons. The information that can be obtained from the magnetic coupling constant is essentially the product μH_{eff}, μ being the nuclear magnetic moment. Assuming the knowledge of the nuclear magnetic moment of Dy^{163} we will, therefore, be able to measure the effective field H_{eff}.

Most available data on nuclear magnetic moments of the rare earths have been obtained indirectly by measuring the hyperfine coupling in paramagnetic salts using magnetic-resonance methods. More or less accurate theoretical estimates of the hyperfine fields then were used to derive the value of the nuclear moment from the experimental data. It is not too surprising to find listed values to scatter by 30% and more. Recently, several direct measurements of nuclear magnetic moments in the rare earth region have been made using atomic beam triple magnetic resonance methods. Table IV summarizes

Table 4. Summary of nuclear magnetic moments of Dy^{161} and Dy^{163}; values are in nuclear magnetons. p.r. means paramagnetic resonance and a.b.r. means atomic beam resonance.

μ		Method	Reference
Dy^{111}	Dy^{113}		
-0.37	$+0.51$	p.r.	4
-0.455	$+0.635$	p.r.	20
0.46	0.65	p.r.	21
-0.47	0.66	a.b.r.	5

some of the pertinent data for the Dy nuclear magnetic moments. The listing of references is by no means complete and is only intended to show the spread of values and the good agreement of recently published data. Most data obtained are from paramagnetic-resonance-measurements, using various assumptions to calculate $\langle r^{-3} \rangle$. The results of PARKS [4] are based on early estimates of $\langle r^{-3} \rangle$ by BLEANEY [19]. Using available paramagnetic-resonance data BLEANEY [20] has recalculated the values for a number of nuclear magnetic moments based on $\langle r^{-3} \rangle$ values obtained by interpolating between some direct nuclear magnetic moment measurements. Recent atomic beam resonance measurements by EBENHÖH et al. [5] are based on the same $\langle r^{-3} \rangle$ values and there is very good agreement between the results. LINDGREN [21] also recalculated earlier paramagnetic-resonance data. His calculations use $4f$ electron wave functions that were adjusted to fit results on Pr^{3+} and Tm^{3+}. Again there is good agreement with the newer measurements. In the following we will use $\mu = +0.66\ \mu_N$ for the moment of Dy^{163} and $\mu = -0.47\ \mu_N$ for Dy^{161}.

The magnetic hyperfine constant in dysposium has been determined previously by several authors using specific-heat methods, NMR and Mössbauer methods, as well as calculations based on magnetic-

[19] B. BLEANEY, Proc. Phys. Soc. London **A 68**, 937 [1955].
[20] B. BLEANEY, Proceedings of the Third International Congress on Quantum Electronics, Paris 1963 (edited by P. GRIVET and N. BLOEMBERGEN), Columbia University Press, New York 1964, p. 595.
[21] I. LINDGREN, Nucl. Phys. **32**, 151 [1962].

Table 5. Comparison of the magnetic hfs results of present work with previously published values. See text for quoted H_{eff} values.

A m Joule deg / mole	CT^2/R $[10^{-4}]$	aJ [Mc/sec] Dy^{161}	Dy^{163}	$a' = A/2k$ [°K] Dy^{161}	Dy^{163}	H_0.. $[10^6$ Oe]	Method	Reference
—	—	825	—	—	—	5,76	Mössbauer	22
—	—	830	—	—	—	5,79	{NMR	23
—	—	—	1163	—	—	5,78	{	
20	—	—	—	—	—	5.06	spec. heat	24
30	—	—	—	—	—	6,19	spec. heat	25
—	26	—	—	—	—	5.26	spec. heat	26
26.4	—	—	—	—	—	5.81	spec. heat	27
—	—	—	—	0.0396	—	5.76	{spec. heat	28
—	—	—	—	—	0.0554	5.73	{	
—	32	—	—	—	—	5.83	spec. heat calc.	29
—	—	820	—	—	—	5.72	{EPR	29
—	—	—	1140	—	—	5.66	{calc.	
—	—	590	—	—	—	4.12	{EPR	30
—	—	—	850	—	—	4.22	{calc.	
—	—	—	—	—	0.0500	5.17	pol. neutron transmission	present work

resonance measurements. Table V summarizes some of these results giving the quoted values for the constants and the effective magnetic field H_{eff}. All values for H_{eff} in Table V were calculated using $\mu = -0.47\ \mu_N$ and $\mu = +0.66\ \mu_N$ for the nuclear magnetic moments of Dy^{161} and Dy^{163}, respectively, and assuming the usual natural abundances of 18.88% and 24.97%, respectively. Previously quoted field values are generally higher because of the lower μ-values used.

Most specific heat measurements were not made to low enough temperatures to determine the electric quadrupole contribution. The analysis was usually complicated further by an anomalous behavior of the specific heat around 2 °K which was shown to be due to sample impurities. However, LOUNASMAA and GUENTHER [27] have analyzed their data using values for the quadrupole interaction calculated by BLEANEY [29]. Recent specific heat measurements by ANDERSON et al. [28] were made down to 0.025 °K yielding values for the quadrupole term in very good agreement with other determinations. The data on the quadrupole interaction are summarized in Table VI. The agreement is in general very good for all values listed.

Table 6. Comparison of the electric hfs results of present work with previously published values.

P [°K] Dy^{161}	Dy^{163}	Method	Reference
0.0077		Mössbauer	22
0.0093		{NMR	23
	0.0098	{	
0.0072		{EPR	29
	0.0086	{calc.	
0.009		{spec. heat	28
	0.010	{	
	0.008	pol. neutron transmission	present work

Acknowledgments

For many years Professor H. MAIER-LEIBNITZ has interacted strongly with the Brookhaven neutron physics research, both directly through his visits and correspondence, and indirectly through the collaborations with many of his former students. These contacts have continually enriched our programs. His creative ideas have proved to be strong stimuli. It has been a privilege and an inspiration to know Professor MAIER-LEIBNITZ. We look forward to his continuing interest and suggestions.

Also we gratefully acknowledge the contributions of Dr. H. L. FOOTE, JR. who designed and supervised the construction of the neutron spectrometer and associated equipment. We are also indebted to Messrs. Robert SCHMIDT, Edward CARUSO, William KRISTIANSEN, and Ronald SMITH for technical support.

[22] S. OFER, M. RAKAVY, E. SEGAL, and B. KHURGIN, Phys. Rev. **138**, A 241 [1965].

[23] S. KOBAYASKI, N. SANO, and J. ITOH, J. Phys. Soc. Japan **21**, 1456 [1966].

[24] J. G. DASH, R. D. TAYLOR, and R. P. CRAIG, Proc. 7th International Conference on Low Temperature Physics, Toronto 1961, p. 705.

[25] B. DREYFUS, B. B. GOODMAN, G. TROLLIET, and L. WEIL, C. R. Acad. Sci. Paris **253**, 1085 [1961]. — B. DREYFUS, B. B. GOODMAN, A. LACAZE, and G. TROLLIET, C. R. Acad. Sci. Paris **253**, 1764 [1961].

[26] R. D. PARKS, Proc. Second Conf. Rare Earth Research, 1961, p. 225.

[27] O. V. LOUNASMAA and R. A. GUENTHER, Phys. Rev. **126**, 1357 [1962].

[28] A. C. ANDERSON, B. HOLMSTRÖM, K. KRUSIUS, and G. R. PICKETT, Phys. Rev. **183**, 546 [1969].

[29] B. BLEANEY, J. Appl. Physics **34**, 1024 [1963].

[30] J. KONDO, J. Phys. Soc. Japan **16**, 1690 [1961].